Time-Resolved Non-Invasive Metabolomic Monitoring of Microfluidic Spheroid And Monolayer Cell Cultures By NMR

Bishnubrata Patra, Manvendra Sharma, William Hale[*], and Marcel Utz[†]

School of Chemistry, University of Southampton, United Kingdom SO17 1BJ

April 17, 2020

Abstract

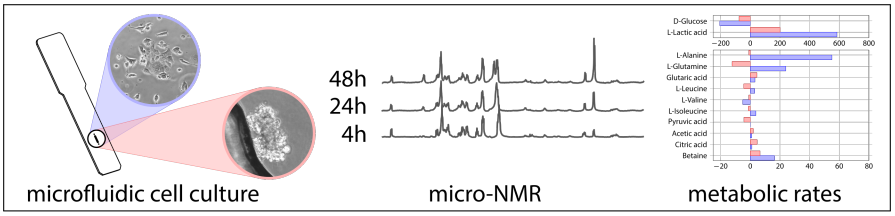

We present a quantitative NMR study comparing the metabolic activity in a spheroid and a monolayer of the same number of MCF-7 cells. Both cultures were carried out under hypoxic conditions on microfluidic devices with 2.5μL sample volume. NMR spectra were obtained by periodically inserting the devices into a dedicated micro-NMR probe. The results demonstrate that quantitative, non-invasive metabolomic monitoring of microfluidic cultures with as few as 1250 individual cells is possible. Metabolite concentrations in the cultures were found to change linearly with time. The consumption rates of D-Glucose and the production rates of L-Lactic acid were approximately 2.5 times larger in the monolayer than in the spheroid. In contrast to the spheroids, monolayers exhibited significant production of L-Alanine and L-Glutamine. Due to its non-invasive nature, metabolic monitoring by NMR can complement destructive fluorescent-based assays that are commonly used for read-out in microfluidic cultures.

v1.1-archive-1-gf832a54

[*]Current address: Department of Chemistry, University of Florida, USA FL 32611-7200

[†]Corresponding Author, marcel.utz@gmx.net

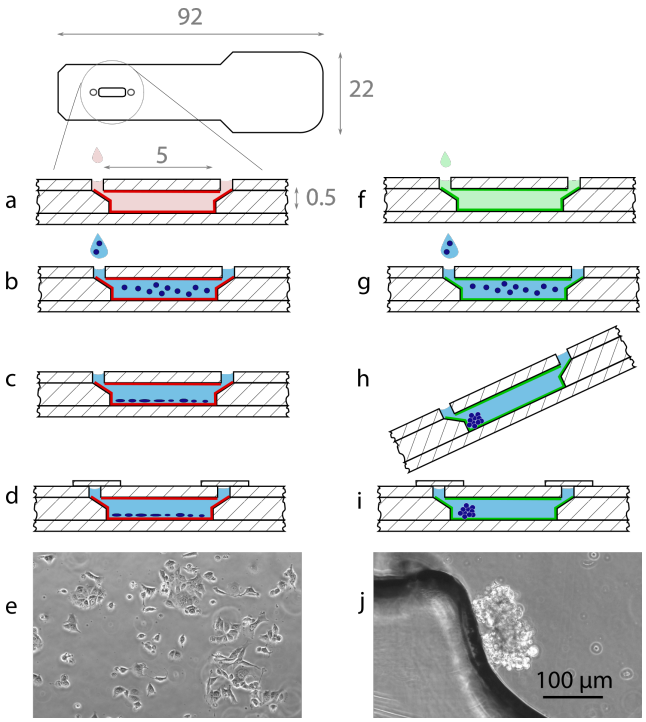

Figure 1: Schematic of the microfluidic device and sample preparation. The device is coated with fibronectin (a, dimensions in mm) or pluronic F-127 (f). Then, cells are seeded in growth medium (b and g), and incubated for 4h (c, h). The pluronic-coated device is held at an angle, allowing the cells to settle at the bottom (h). Finally, the devices are sealed with adhesive tape (d, i). Phase contrast micrograph of the adherent monolayer (e) and spheroid culture (j).

Microfluidic lab-on-a-chip (LoC) devices are increasingly finding applications in chemistry and the life sciences. They allow efficient experimentation with very small sample volumes, high throughput, and convenient integration of multiple experimental steps onto a single, compact platform. Another advantage lies in the detailed control over the conditions of growth in the culture of cells, spheoids, tissues, and small organisms. This enables systematic comparisons of the effect of different parameters on growth and development. Examples include studies of tumour growth and vascularisation [1], the response of cells to inflammatory agents [2], liver toxicity of drugs [3], and the differentiation of induced pluripotent stem cells into functional tissues [4]. In most microfluidic studies, information is extracted from the LoC device in a destructive end-point analysis through a fluorescence based assay. This can take the form of micro-PCR based genomic or transcriptomic analysis, proteomics by western blot, or an immunoassay targeting a small set of specific biomarkers. In addition, it would be very useful to follow the metabolism of such culture systems longitudinally, i.e., over the course of the entire

experiment. This would allow to correlate metabolic activity during the culture with the results of the destructive end-point analysis. NMR spectroscopy is uniquely suited for metabolomic observation of live systems, since it is non-invasive, label-free, and allows for direct quantitation of analytes. The small sample volumes involved in microfluidic systems, however, pose a challenge in terms of sensitivity. Highly efficient NMR micro-detectors have been developed by a number of groups over the past two decades [5–12] and sensitivities in the vicinity of 1 nmol $\sqrt{\text{s}}$ have been achieved with samples around 1 μL volume [13]. Our group have recently presented a modular microfluidic NMR system that accommodates generic LoC devices [14]. In the present contribution, we show that this makes it possible to quantitatively follow the metabolic activity of as few as 1250 mammalian cells in 2.5 μL of medium over the course of 48h. At the same time, the LoC approach allows convenient control over the culture conditions. In the present study, this is exploited for a quantitative comparison of the metabolic activity of the same number and type of cells grown (i) in monolayer adherent to the chip surface and (ii) as a spheroid.

Spheroids provide an intermediate between conventional two-dimensional monolayer culture of adherent cells and primary tissue culture. Spheroids model at least some of the three-dimensional aspects of inter-cellular organisation, as well as 3D transport of nutrients, oxygen, and intercellular signals [15]. They are widely used as models for cancer in both translational and fundamental research [16]. Microfluidic LoC devices for spheroid culture need to prevent cell adhesion to the chip surface. This has been accomplished using the air/liquid interface in hanging drops [17–19], as well as in enclosed chambers with appropriate coatings [20].

NMR is a powerful tool to study metabolic differences between monolayer and spheroid cell culture. At the macro scale, Santini et al. have studied MG-63 human osteosarcoma cells grown in monolayer and spheroids using a conventional NMR set up and observed the difference in metabolic activity [21] by ^{1}H NMR spectroscopy of cells and perchloric acid cell extracts. The study was limited to a single time point observation, and a very large number of cells was used (order of 10^8). Real-time monitoring of cells using NMR provides a critical step for understanding cellular metabolism. For example, Pilatus et al. have used cells attached on polystyrene microbeads to study oxygen consumption, pH and energy metabolism using NMR spectroscopy [22]. Recently, Wen et al. studied the metabolism of cancer cells vs normal cells in suspension and the effect of an anticancer agent was observed [23]. While studies on large numbers of spheroids provide averaged information of spheroid metabolism, they do

not capture the variability between spheroids. In addition, single spheroid capability would enable high-throughput combinatorial studies of the effects of drugs and culture conditions. Single-spheroid metabolomics has been achieved using mass spectrometry [24], but this is a destructive end-point analysis.

Kalfe et al. have demonstrated that it is possible to obtain metabolic information from a single spheroid (diameter 0.5 mm with 9000 cells) [25], by combining microfluidic and micro-NMR technology. However, the setup used in [25] involved a dedicated fluidic design that provides continuous nutrient supply to the spheroid via evaporation-driven convection. This makes it difficult to derive quantitative metabolic consumption/production rates. It is also not possible to change the experimental modality, for example to compare the metabolism of spheroids with adherent monolayers of the same cell type. More recently, Palma et al. have studied the effect of irradiation on monolayers and spheroids of MCF-7 breast cancer cells by NMR spectroscopy of cell suspensions, as well as by micro-NMR imaging of individual spheroids [26]. However, the spectral resolution was very limited, and while the results showed interesting trends, no truly quantitative information was obtained from individual spheroids.

In the present study, we demonstrate that a flexible microfluidic NMR platform can be used to quantitatively compare metabolic data obtained under different experimental modalities. The platform consists of a modular transmission line NMR micro-probe [14] in combination with disposable, generic LoC devices. Human adenocarcinoma cells (MCF-7) [27] were cultured under hypoxic conditions in LoC devices which were coated either with fibronectin, in order to promote adhesion of the cells to the chip surface [28], or with pluronic F-127, which prevents cell adhesion and forces the cells to form a spheroid [29]. After seeding, the cells were incubated at 37°C. At regular intervals, the LoC devices were removed from the incubator, inserted into the NMR spectrometer for a 15 min measurement, micrographed, and returned to the incubator. After 48h, the viability of the cells was tested using a fluorescent live/dead stain. As will be discussed in detail in the following, the study reveals significant differences in the metabolic activity of the same cells between monolayer and spheroid culture.

Microfluidic chips made from polymethyl methacrylate (PMMA) with culture chambers of 2.5 μL volume [30] were coated with either fibronectin or with pluronic F-127 (Fig. 1a and f). The former promotes cell adhesion [31, 32], while the latter is a polyethylene oxide / poly propylene / polyethylene oxide block copolymer which is well known to prevent protein and cell adhesion [33, 34]. Each chip was seeded with a suspension of 2.5 μL of MCF-7 cells in

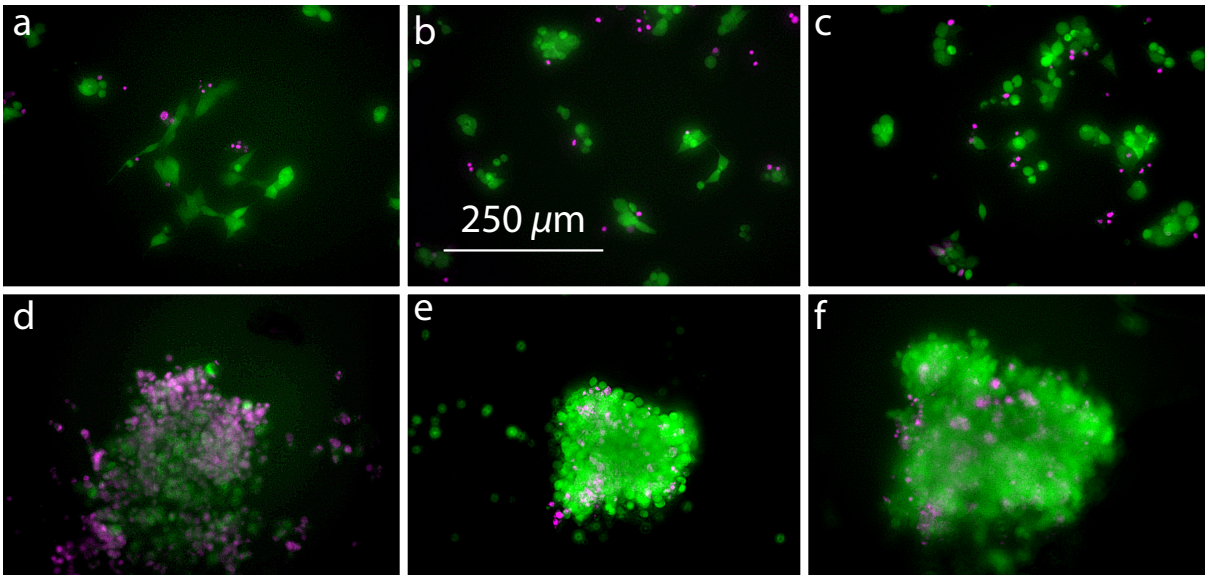

Figure 2: Live(green)/dead(purple) stain of MCF-7 cells cultured under hypoxic conditions in an adherent monolayer (a-c) and as a spheroid (d-f) after 48h. The seeding density increases from left to right with 500 cells/μL (a and d), 750 cells/μL (b and e), and 1000 cells/μL (c and f).

culture media (Fig. 1b and g), and was allowed to incubate for 4h at 37°C. During this time, the pluronic-coated chips were kept at an angle (Fig. 1h), causing the cells to settle near the bottom of the culture chamber, while the fibronectin-coated chips were kept lying flat. This led to formation of an adherent monolayer of cells in the culture chamber at less than 20% confluence in the case of fibronectin-coated devices, and to formation of a cell spheroid in the ones coated with pluronic F-127, as shown in Fig. 1e and j, respectively. The chips were then sealed with an airtight self-adhesive film, and were transferred to an incubator at 37°C for a further 44h. At regular intervals, the chips were removed from the incubator and inserted into a NMR spectrometer operating at a proton Larmor frequency of 600 MHz using a specially built transmission line micro-NMR probe [14]. The ^{1}H NMR spectrum of the entire 2.5μL culture volume on each chip was recorded using water presaturation and a T_2 filter [35] (15 min total acquisition time), a phase contrast micrograph was taken, and the chip was then returned to the incubator. After 48h, the viability of the cells in each device was assessed using a fluorescent live/dead stain, as shown in Fig. 2.

After 48h, the monolayer cultures (Fig. 2a-c) show generally good viability, with only a small number of dead cells visible in each case. Cell spheroids are shown in Fig. 2d-f. At the

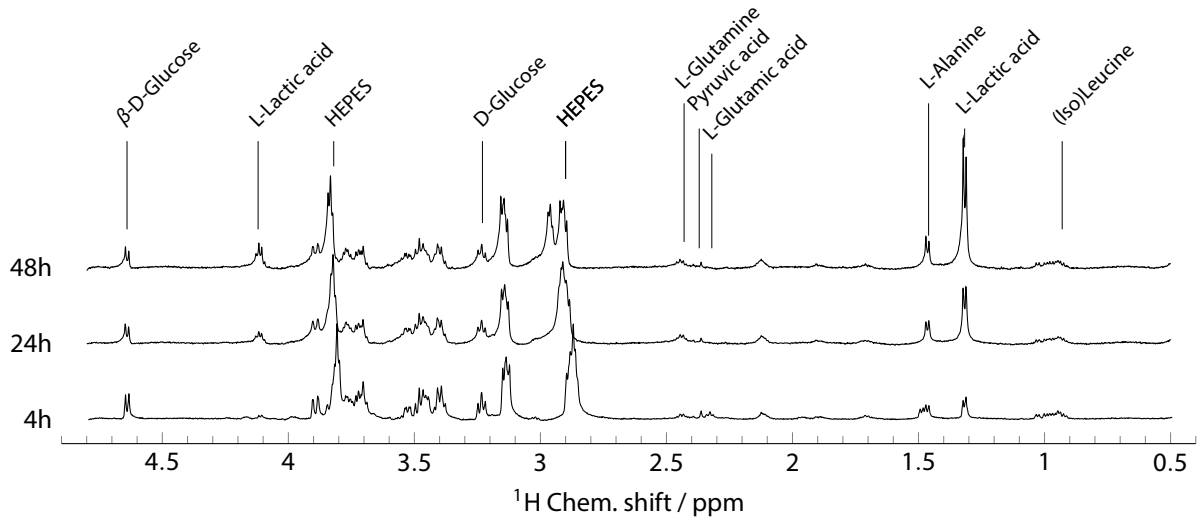

Figure 3: 600 MHz ^{1}H NMR spectra from a spheroid of about 2000 cells (obtained at a seeding density of 1000 cells/μL) after 4h, 24h, and 48h of culture.

lowest seeding density, only a loose spheroid is obtained, and cell viability at the end of the experiment is poor. By contrast, the higher seeding densities lead to a compact spheroid with only a small number of dead cells present after 48h (Fig. 2e and f).

^{1}H NMR spectra and micrographs were taken from each chip at 4h, 8h, 24h, 32h, and 48h after cell seeding. In addition, controls without cells were also run at the same time points (SI). The entire experiment was run three times with newly made microfluidic devices, resulting in a collection of more than 100 individual NMR spectra. Fig. 3 shows three of these NMR spectra obtained from a spheroid at 4h, 24h, and 48h of culture. The spectra exhibit a resolution of about 3 Hz; the signal/noise ratio is about 200 based on the HEPES peak at 3.82 ppm. The most obvious change over time is the growth of the L-Lactic acid doublet at 1.32 ppm. The same effect is also visible in the monolayer culture (data not shown), but at significantly larger magnitude. At the same time, the HEPES signals exhibit gradual shifts which reflect changes in pH. For example, a peak at 2.85 ppm at 4h of culture in Fig. 3 shifts to 2.95 ppm at 48h. These shifts can be calibrated to give a quantitative pH reading. Fig. 4 summarises the evolution of the pH in the growth medium, obtained from the HEPES peak at 3.8 ppm (calibration given in the SI).

More detailed inspection of the spectra reveals a range of additional systematic changes over time. These reflect changes in metabolite concentrations in the culture medium (exa-metabolome). In order to quantify metabolite concentrations, the spectra were processed in Julia

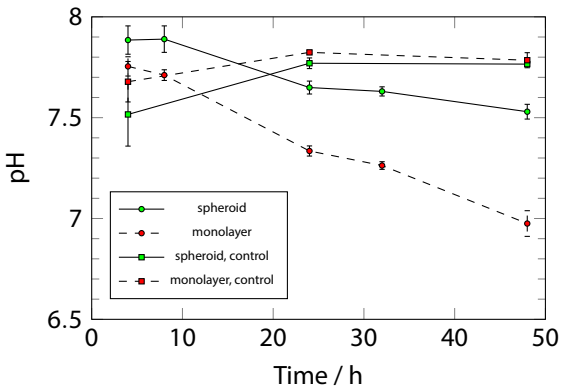

Figure 4: Evolution of pH in the growth medium over 48h of culture, as obtained from the chemical shift of the HEPES peak near 3.8 ppm. Red symbols: monolayer culture (fibronectin coated devices); Green symbols: spheroid culture (pluronic F-127 coated devices). The circles represent cultures with about 2000 cells (seeding density of 1000 cells/μL); the squares are controls without cells. Solid and dashed lines are guides to the eye.

[36] using a model-free approach, which is described in detail in the supporting information. Briefly, a list of peak positions, intensities, and widths is derived from each spectrum. This list is then compared with all available proton NMR peak lists in the human metabolome database (https://hmdb.org) [37]. For each metabolite in the database, a score is calculated based on how many of its expected peaks can be identified in the spectrum, where missing peaks are counted negative. The metabolites were then listed in order of decreasing score. The 12 metabolites that occurred within the top 25 list for all spectra were selected for quantitative analysis.

The spectra were normalised in intensity with respect to the HEPES buffer peak at approximately 3.8 ppm. They were then projected onto a set of metabolite reference spectra obtained from the human metabolome database. This yields an intensity value for each metabolite, which is then converted to an absolute concentration using the known D-Glucose concentration in the control experiments as a standard. Fig. 5 shows the evolution of the concentration of several metabolites as a function of time for the monolayer cells and for the spheroid. The error bars represent twice the standard error of the mean for three separate experiments, which had been carried out over the course of three months, and involved newly fabricated chips and new cells each time. The excellent repeatability of these results demonstrates the stability of the method and the reliability of the NMR data for quantitative interpretation.

The observed concentrations of D-Glucose and L-Lactic acid change linearly with time

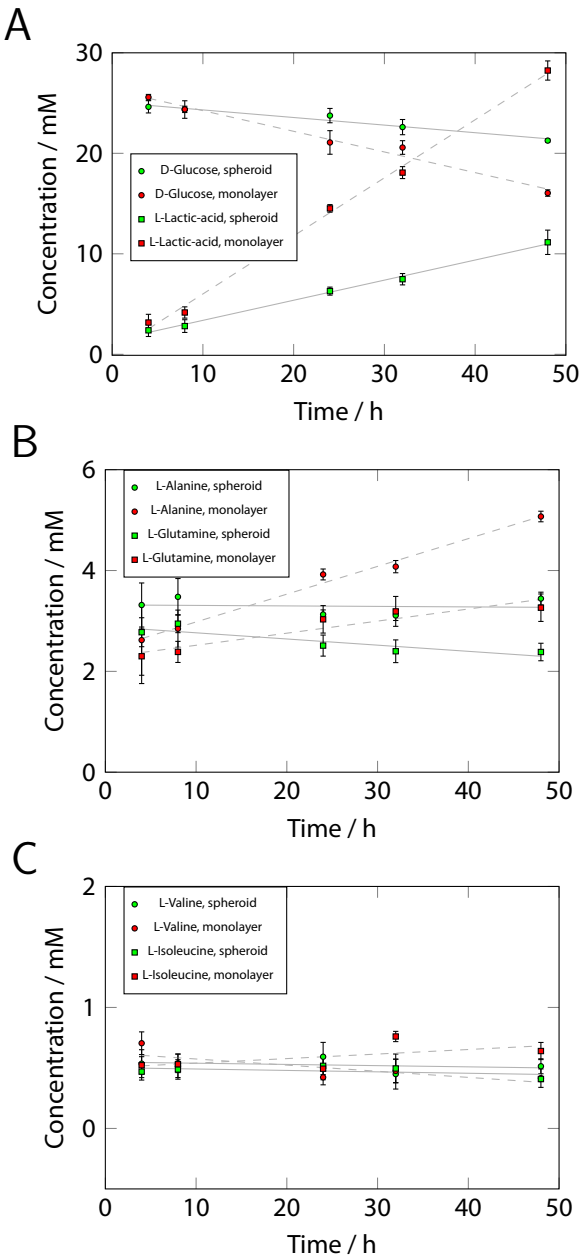

Figure 5: Metabolite concentrations over time in monolayer (red symbols, dashed lines) and spheroid culture (green symbols, solid lines). Each sample contained about 2000 cells; seeding density was 1000 cells/μl in all cases. Error bars represent twice the standard error of the mean, $n = 3$.

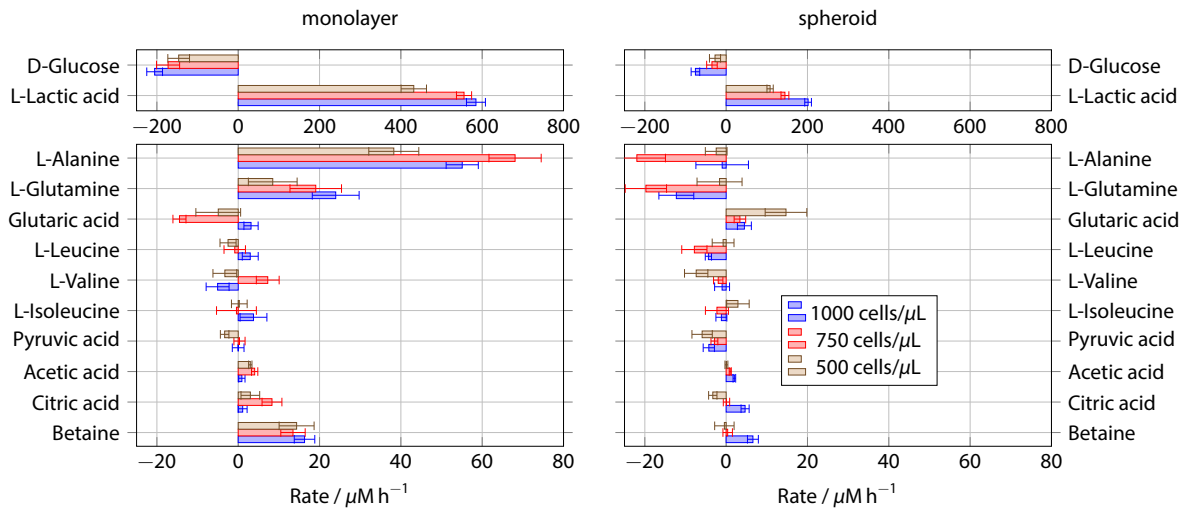

Figure 6: Production (positive) or consumption (negative) rates of different metabolites as determined from the NMR spectra for monolayer (left) and spheroid culture (right).

within experimental precision, as shown by the regression lines in Fig. 5A. The monolayer cells consume D-Glucose significantly faster than the spheroids, and their L-Lactic acid production is correspondingly higher by a factor of about 2.5. Fig. 5B shows the concentrations of L-Alanine and L-Glutamine. While the response of the spheroid and monolayer cultures is similar in the case of D-Glucose and L-Lactate apart from the nearly threefold difference in consumption/production rate, there is a qualitative difference in the cases of L-Alanine and L-Glutamine. While spheroids do not seem to produce detectable amounts of L-Alanine, there is a clear linear increase in the L-Alanine concentration from 2 mM to 5 mM in the monolayer culture over 44h. The monolayer cells also seem to produce L-Glutamine, while the L-Glutamine concentration shows a slightly decreasing trend in the case of the spheroid culture. It is known that MCF-7 cells can produce L-Glutamine [38], and it has been speculated that hypoxic conditions lead to upregulation of L-Glutamine synthetase and downregulation of glutaminases [26]. Our results suggest that while this effect is visible in the monolayer culture, it is largely absent in the cell spheroids. Finally, most other metabolites seem to remain at constant concentrations within experimental error; L-Valine and isoleucine are shown in Fig. 5C as examples.

The full set of data obtained can be visualised in terms of the rates of change in metabolite concentrations, as shown in Fig. 6. Results from experiements at all three seeding densities are shown here; the plots in Fig. 5 only correspond to 1000 cells/μL. The D-Glucose consumption rate of the monolayers at the highest seeding density amounts to about 200 μM h^{-1}. The number

of cells in the device were determined by image analysis (SI) to 2000±300 cells. In a 2.5μL culture volume, this corresponds to a D-Glucose consumption rate of 250 fmol h^{-1} per cell. Similarly, the L-Lactic acid production rate is 550 μM h^{-1}, corresponding to 687 fmol h^{-1} per cell. The metabolic activity of MCF-7 cells in monolayer culture has been determined as a function of oxygen partial pressure in a macroscopic experiment ($> 10^6$ cells) using radiotracers by Guppy et al [39]. They found that the L-Lactic acid production rate steeply falls with oxygen concentration; at 5 μM oxygen, they obtained a value of 800 fmol h^{-1} per cell, which rose to just over 1000 fmol h^{-1} per cell at 0 μM oxygen. The value obtained here is slightly lower, which may be due to oxygen leakage into the chip resulting in a residual oxygen concentration somewhat above 5 μM. The metabolic rate of the spheroids is shown on the right side of Fig. 6. Their rates of D-Glucose consumption and L-Lactic acid production are a factor of 2.5 smaller than in monolayer culture. To our knowledge, this is the first quantitative determination of the metabolic rate of an individual spheroid of MCF-7 cells. The ratio between the rate of L-Lactic acid production and D-Glucose consumption is more than 2 in all cases (cf. Fig. 6). However, Stoichiometry would dictate that each molecule of D-Glucose can be converted at most into two molecules of L-Lactic acid. This surprising finding is not due to measurement error, since a calibration experiment with a sample of known D-Glucose and L-Lactic acid concentration (SI) showed that the D-Glucose/L-Lactic acid concentration ratio obtained by NMR is accurate to within 10%. At this point, we do not have an explanation for this surprising phenomenon. Possibly, there is another source for the excess amount of L-Lactic acid which is not visible to the liquid NMR measurement, for example D-Glucose contained a priori within the cells.

In conclusion, the above results show that microfluidic NMR can provide a flexible platform for the quantitative and non-invasive study of the metabolism of cultures of cells and spheroid. Consumption/production rates of the most abundant metabolites can be determined accurately from as few as 1250 cells. For MCF-7 cells, the metabolic rates of D-Glucose and L-Lactic acid are a factor of 2.5 larger in monolayer culture than in spheroids.

Acknowledgements

The datasets generated during and/or analysed during the current study are available in the University of Southampton Institutional repository (`https://doi.org/doi:10.5258/SOTON/D1329`). We thank Ms. Sylwia Ostrowska and Mr. Jacob Keeley for help with the pH calibration and for performing a T_1 measurement of the growth medium. This work was supported by the European

Commission through the Horizon 2020 Future and Emerging Technologies programme, Project TISuMR (Grant number 737043).

Keywords: Cell culture, microfluidics, metabolomics, single-spheroid NMR

References

[1] S. Kim, W. Kim, S. Lim, J. S. Jeon, *Bioengineering* **2017**, *4*, 8.

[2] M. Junkin, S. Tay, *Lab on a Chip* **2014**, *14*, 1246–1260.

[3] P. M. van Midwoud, E. Verpoorte, G. M. Groothuis, *Integrative Biology* **2011**, *3*, 509–521.

[4] A. D. Gracz, I. A. Williamson, K. C. Roche, M. J. Johnston, F. Wang, Y. Wang, P. J. Attayek, J. Balowski, X. F. Liu, R. J. Laurenza, L. T. Gaynor, C. E. Sims, J. A. Galanko, L. Li, N. L. Allbritton, S. T. Magness, *Nature Cell Biology* **2015**, *17*, 340–349.

[5] N. Wu, T. L. Peck, A. G. Webb, R. L. Magin, J. V. Sweedler, *Analytical Chemistry* **1994**, *66*, 3849–3857.

[6] R. Subramanian, M. M. Lam, A. G. Webb, *Journal of Magnetic Resonance* **1998**, *133*, 227–231.

[7] C Massin, F Vincent, A Homsy, K Ehrmann, G Boero, P. Besse, A Daridon, E Verpoorte, N. de Rooij, R. Popovic, *Journal of Magnetic Resonance* **2003**, *164*, 242–255.

[8] J. Bart, A. J. Kolkman, A. J. Oosthoek-de Vries, K. Koch, P. J. Nieuwland, H. J. W. G. Janssen, P. J. M. van Bentum, K. A. M. Ampt, F. P. J. T. Rutjes, S. S. Wijmenga, H. J. G. E. Gardeniers, A. P. M. Kentgens, *Journal Of The American Chemical Society* **2009**, *131*, 5014–5015.

[9] K. Kratt, V. Badilita, T Bürger, J. G. Korvink, U. Wallrabe, *J. Micromech. Microeng.* **2009**, *20*, 015021.

[10] H. Ryan, S.-H. Song, A. Zaß, J. Korvink, M. Utz, *Analytical Chemistry* **2012**, *84*, 3696–3702.

[11] R. M. Fratila, M. V. Gomez, S. Sýkora, A. H. Velders, *Nature Communications* **2014**, *5*, 1–8.

[12] N Spengler, A Moazenzadeh, R. C. Meier, V. Badilita, J. G. Korvink, U. Wallrabe, *J. Micromech. Microeng.* **2014**, *24*, 034004.

[13] G. Finch, A. Yilmaz, M. Utz, *Journal of Magnetic Resonance* **2016**, *262*, 73–80.

[14] M. Sharma, M. Utz, *Journal of Magnetic Resonance* **2019**, *303*, 75–81.

[15] M. Huch, J. A. Knoblich, M. P. Lutolf, A. Martinez-Arias, *Development* **2017**, *144*, 938–941.

[16] S. F. Boj, C.-I. Hwang, L. A. Baker, I. I. C. Chio, D. D. Engle, V. Corbo, M. Jager, M. Ponz-Sarvise, H. Tiriac, M. S. Spector, A. Gracanin, T. Oni, K. H. Yu, R. van Boxtel, M. Huch, K. D. Rivera, J. P. Wilson, M. E. Feigin, D. Öhlund, A. Handly-Santana, C. M. Ardito-Abraham, M. Ludwig, E. Elyada, B. Alagesan, G. Biffi, G. N. Yordanov, B. Delcuze, B. Creighton, K. Wright, Y. Park, F. H. M. Morsink, I. Q. Molenaar, I. H. Borel Rinkes, E. Cuppen, Y. Hao, Y. Jin, I. J. Nijman, C. Iacobuzio-Donahue, S. D. Leach, D. J. Pappin, M. Hammell, D. S. Klimstra, O. Basturk, R. H. Hruban, G. J. Offerhaus, R. G. J. Vries, H. Clevers, D. A. Tuveson, *Cell* **2015**, *160*, 324–338.

[17] O. Frey, P. M. Misun, D. A. Fluri, J. G. Hengstler, A. Hierlemann, *Nature Communications* **2014**, *5*, 1–11.

[18] S. R. Yazdi, A. Shadmani, S. C. Bürgel, P. M. Misun, A. Hierlemann, O. Frey, *Lab on a Chip* **2015**, *15*, 4138–4147.

[19] P. M. Misun, J. Rothe, Y. R. F. Schmid, A. Hierlemann, O. Frey, *Microsystems & Nanoengineering* **2016**, *2*, 1–9.

[20] B. Patra, Y.-H. Chen, C.-C. Peng, S.-C. Lin, C.-H. Lee, Y.-C. Tung, *Biomicrofluidics* **2013**, *7*, 054114.

[21] M. T. Santini, G. Rainaldi, R. Romano, A. Ferrante, S. Clemente, A. Motta, P. L. Indovina, *FEBS letters* **2004**, *557*, 148–154.

[22] U. Pilatus, E. Aboagye, D. Artemov, N. Mori, E. Ackerstaff, Z. M. Bhujwalla, *Magnetic Resonance in Medicine: An Official Journal of the International Society for Magnetic Resonance in Medicine* **2001**, *45*, 749–755.

[23] H. Wen, Y. J. An, W. J. Xu, K. W. Kang, S. Park, *Angewandte Chemie International Edition* **2015**, *54*, 5374–5377.

[24] M. Acland, P. Mittal, N. A. Lokman, M. Klingler-Hoffmann, M. K. Oehler, P. Hoffmann, *PROTEOMICS–Clinical Applications* **2018**, *12*, 1700124.

[25] A. Kalfe, A. Telfah, J. Lambert, R. Hergenröder, *Analytical chemistry* **2015**, *87*, 7402–7410.

[26] A. Palma, S. Grande, A. M. Luciani, V. Mlynárik, L. Guidoni, V. Viti, A. Rosi, *Frontiers in Oncology* **2016**, *6*, DOI 10.3389/fonc.2016.00105.

[27] K. B. Horwitz, M. E. Costlow, W. L. McGuire, *Steroids* **1975**, *26*, 785–795.

[28] E. Ruoslahti, *Cancer and Metastasis Reviews* **1984**, *3*, 43–51.

[29] J. Treter, F. Bonatto, C. Krug, G. V. Soares, I. J. R. Baumvol, A. J. Macedo, *Applied Surface Science* **2014**, *303*, 147–154.

[30] A. Yilmaz, M. Utz, *Lab on a Chip* **2016**, *16*, 2079–2085.

[31] J. M. Anderson, N. P. Ziats, A. Azeez, M. R. Brunstedt, S. Stack, T. L. Bonfield, *Journal of Biomaterials Science Polymer Edition* **1996**, *7*, 159–169.

[32] H. Lu, L. Y. Koo, W. M. Wang, D. A. Lauffenburger, L. G. Griffith, K. F. Jensen, *Analytical Chemistry* **2004**, *76*, 5257–5264.

[33] M. Amiji, K. Park, *Biomaterials* **1992**, *13*, 682–692.

[34] J. Treter, F. Bonatto, C. Krug, G. V. Soares, I. J. R. Baumvol, A. J. Macedo, *Applied Surface Science* **2014**, *303*, 147–154.

[35] J. A. Aguilar, M. Nilsson, G. Bodenhausen, G. A. Morris, *Chemical Communications* **2011**, *48*, 811–813.

[36] J. Bezanson, A. Edelman, S. Karpinski, V. B. Shah, *SIAM Review* **2017**, *59*, 65–98.

[37] D. S. Wishart, Y. D. Feunang, A. Marcu, A. C. Guo, K. Liang, R. Vázquez-Fresno, T. Sajed, D. Johnson, C. Li, N. Karu, Z. Sayeeda, E. Lo, N. Assempour, M. Berjanskii, S. Singhal, D. Arndt, Y. Liang, H. Badran, J. Grant, A. Serra-Cayuela, Y. Liu, R. Mandal, V. Neveu, A. Pon, C. Knox, M. Wilson, C. Manach, A. Scalbert, *Nucleic Acids Research* **2018**, *46*, D608–D617.

[38] H.-N. Kung, J. R. Marks, J.-T. Chi, *PLOS Genetics* **11-Aug-2011**, *7*, e1002229.

[39] M. Guppy, S. Brunner, M. Buchanan, *Comparative Biochemistry and Physiology Part B: Biochemistry and Molecular Biology* **2005**, *140*, 233–239.

Entry for the Table of Contents

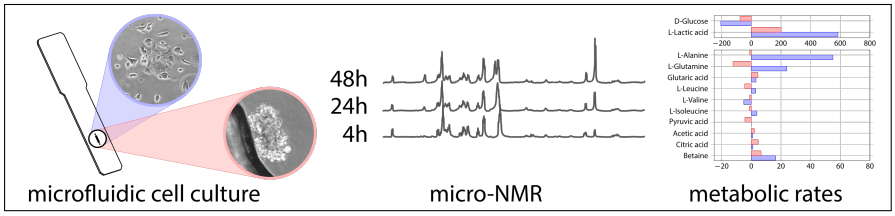

Integrating microfluidic cell culture with NMR spectroscopy provides quantitative information on metabolic rates from as few as 1250 cells. In this study, we compare the metabolism of a single spheroid to a monolayer of the same human cells.

Twitter handle: `@UtzGroup`